Research

Stochastic Mixed-Integer Branch Flow Optimization for the Optimal Integration of Fixed-Step Capacitor Banks in Electrical Distribution Grids

Optimización estocástica, entera mixta y de flujo por ramas para la integración óptima de bancos de capacitores de paso fijo en redes de distribución de energía

Walter Gil-González [ID] [✉]*, Andrés Herrera-Orozco [ID], Alexander Molina-Cabrera [ID],

Department of Electrical Engineering, Universidad Tecnológica de Pereira, Pereira 660003, Colombia. [ROR]

Abstract

Context: The use of capacitor banks is the most common and preferred solution for reducing power losses in electrical distribution networks, given their cost-effectiveness and low maintenance requirements. However, achieving their optimal integration in terms of location and size is a challenging problem.

Method: This paper proposes a stochastic mixed-integer convex model based on a branch flow optimization model, which incorporates three different load-generation conditions, in order to address the stochastic nature of distribution systems.

Results: The simulation results indicate that the proposed stochastic mixed-integer branch flow (SMIBF) model provides the best solution for all test feeders analyzed, reducing the objective function value by 39,81, 35,29, and 56,31 % regarding the benchmark case in the modified 33-, 69-, and 85-node test feeders, respectively.

Conclusions: An SMIBF model was developed to optimally integrate fixed-step capacitor banks into electrical distribution grids. This model considered the stochastic nature of distribution systems under multiple operating conditions and ensured that the global optimum could be found.

Keywords: stochastic mixed-integer model, branch flow optimization, fixed-step capacitor banks, electrical distribution network, global optimum

---

*✉ **Correspondence:** wjgil@utp.edu.co

Resumen

Contexto: El uso de bancos de capacitores es la solución más común y preferida para reducir la pérdida de energía en redes de distribución eléctrica, dados su rentabilidad y bajos requisitos de mantenimiento. Sin embargo, lograr su integración óptima en términos de ubicación y tamaño es un problema desafiante.

Métodos: Este artículo propone un modelo convexo estocástico entero-mixto basado en un modelo de optimización de flujo de ramas, el cual incorpora tres diferentes condiciones de generación-carga, para abordar la naturaleza estocástica de los sistemas de distribución.

Resultados: Los resultados de la simulación indican que el modelo SMIBF propuesto proporcionó la mejor solución para todos los sistemas de prueba analizados, reduciendo el valor de la función objetivo en un 39,81, 35,29 y 56,31 % respecto al caso de referencia para los alimentadores de prueba modificados de 33, 69 y 85 nodos respectivamente.

Conclusiones: Se desarrolló un modelo SMIBF para la integración óptima de bancos de capacitores de paso fijo en redes de distribución eléctrica. Este modelo tuvo en cuenta la naturaleza estocástica de los sistemas de distribución bajo múltiples condiciones de operación y garantizó que se pudiera encontrar el óptimo global.

Palabras clave: modelo estocástico de enteros mixtos, optimización de flujo de ramas, bancos de capacitores de paso fijo, red de distribución eléctrica, óptimo global

Table of contents

Nomenclature

Acronyms

AC   Alternating current.

EDN   Electrical distribution network.

GAMS   General Algebraic Modeling System.

MINLP Mixed-integer nonlinear programming.

OF   Objective function.

PV   Photovoltaic.

SMIBF   Stochastic mixed-integer branch flow.

Parameters

ζ_s Probability factor for scenario s.

A_k Node-to-branch incident matrix for node k.

$C_{\text{cap}}^{\text{máx}}$ Maximum costs associated with capacitor bank installation ($USD).

$C_{\text{loss}}^{\text{máx}}$ Maximum annual cost of energy losses ($USD).

K_p Cost factor of the annual energy losses ($USD/kVA).

K_t Cost factor of the capacitor banks ($USD/kvar-year).

N^{cap} Maximum number of capacitor banks.

$p^{\text{mín}}, p^{\text{máx}}$ Minimum and maximum power from renewable energy sources (W).

Q_t Nominal power of the capacitor bank type t (kVA).

R_l Resistive effect of the transmission line l (Ω).

$v^{\text{mín}}, v^{\text{máx}}$ Minimum and maximum voltage limits (V).

X_l Reactance effect of the transmission line l (Ω).

Sets and Indices

$\mathcal{B}$ Set of network branches.

$\mathcal{N}$ Set of network nodes.

$\mathcal{S}$ Set of scenarios.

$\mathcal{T}$ Set of capacitor bank types.

k, m Node indices ($k, m \in \mathcal{N}$).

l Branch indices ($l \in \mathcal{B}$).

t Capacitor bank type ($t \in \mathcal{T}$).

Variables

ω Weighting factor.

I_l Squared magnitude of the current at branch l (A^2).

i_l Magnitude of the current flowing through transmission line l (A).

$p_{k,dg}$ Active power generated via renewable energy sources at node k (W).

$p_{k,d}$ Active power demanded at node k (W).

P_l Active power flow vector of the branches (W).

p_l Active power flow of branch l (W).

$q_{k,d}$ Reactive power demanded at node k (var).

$Q_{k,t}$ Reactive power delivered by the capacitor bank connected to node k (kvar).

Q_l Reactive power flow vector of the branches (var).

q_l Reactive power flow of branch l (var).

V_k Squared magnitude of the voltage at node k (V^2).

$v_m or (v_k)$ Magnitude of the voltage at node m (or k) (V).

y_{kt} Binary variable that selects the type of capacitor t connected at node k.

z Objective function ($USD).

z_1 Annual costs of energy loss ($USD).

z_2 Costs associated with capacitor bank installation ($USD).

1. Introduction

Electrical distribution networks (EDNs) supply electricity to both rural and urban areas at medium- and low-voltage levels (1). These networks are usually designed with a radial topology, which helps reduce costs for conductors and infrastructure, and simplifies the implementation and coordination of protection schemes (2). Nevertheless, radial EDNs entail significant energy losses, as there is only one line to carry electrical energy from the generation point (substation) to each demand node. Generally, energy losses in radial EDNs are within the range of 6 to 18 % of all the power delivered by the generator at the substation, whereas, in transmission systems, energy losses are approximately 2 % (3).

Utility companies have various options to address the issue of power losses in EDNs. These include making changes to the network's topology and connecting shunt devices (4–6). In the case of topology changes, additional transmission lines are used, which connect to or are disconnected from the electrical system to minimize power losses for specific load conditions while maintaining their radial topologies (7). As for the incorporation of shunt systems, the following technologies have been used: distributed generator systems (*e.g.*, solar and wind energy sources) (8), distribution network flexible AC transmission system (D-FACTS) devices (*e.g.*, distribution static power compensators, or D-STATCOMs, static Var compensators, or SVCs, and fixed-step capacitor banks) (9, 10), and energy storage systems such as batteries (11). However, some of these systems are expensive when it comes to only reducing power losses, which does not allow recovering the investment made (*e.g.*, distributed generator systems and energy storage systems). As a result, it is necessary to consider other objectives to justify their installation (11). The dispatch of reactive power can reduce the power losses in EDNs. Hence, systems such as D-FACTS or fixed-step capacitor banks are ideal. Capacitor banks are cheaper compared to distribution static compensators, require minimal maintenance, have a lifespan of over 25 years (12), and are highly reliable (13). Therefore, capacitors are considered to be the most reliable and cost-effective strategy for reducing power losses (10).

Capacitor banks have long been used as a solution to reduce energy losses in EDNs (10), and determining their optimal locations and sizes is of great importance. The problem lies in their mathematical model, which is challenging to solve because it includes two sets of variables (integer and binary). This implies a model with a mixed-integer nonlinear programming (MINLP) structure (14). The variables for the location and size of the new capacitor banks are binary, while the remaining problem variables are continuous. These include voltage profiles, generated and demanded apparent power, and apparent power flows, among others.

Combinatorial methods are commonly used to find a solution for the non-convex MINLP model that determines the location and size of capacitor banks in EDNs. The most relevant methods in this regard are listed below.

The study by (10) used the flower pollination method to effectively select the sizes and positions of fixed-step capacitor banks in radial EDNs. The goal was to reduce the annual operating costs of the grid, which include energy losses and the investments made in capacitors. The flower pollination

method was evaluated in four EDNs with 33, 34, 69, and 85 nodes. The simulation results indicated that the proposed method yielded superior solutions when compared to other approaches, including analytical sensitivity methods, fuzzy logic algorithms, and classical genetic algorithms.

The work by (15) suggested using a discrete version of the vortex search approach to find and select suitable fixed-step capacitor banks for installation in EDNs. This work conducted numerical experiments on two well-known test systems consisting of 33 and 69 nodes. The findings indicated that the proposed approach was superior to the flower pollination algorithm in terms of efficiency.

The authors of (16) solved the problem regarding the optimal siting and sizing of capacitor banks in EDNs using the well-known General Algebraic Modeling System (GAMS) software. The authors improved the simulation results by incorporating the classical Chu & Beasley genetic methodology. They used two well-known test systems (33 and 69 nodes) and highlighted that the methodology could handle both EDN topologies (radial and meshed) without any modification.

Another study (17) introduced a heuristic approach for locating and sizing capacitor banks in EDNs. Its primary contribution the full incorporation of grid harmonic distortion into the heuristic optimization approach. This study utilized three IEEE test systems to demonstrate that the proposed algorithm could effectively decrease the total grid costs, surpassing the classical genetic algorithm.

The study by (18) proposed a bi-level methodology for solving the mathematical model for the optimal integration (siting and sizing) of fixed-step capacitor banks in radial EDNs. This methodology consisted of combining the generalized normal distribution algorithm with the optimal power flow method. The latter used a linearization of the power flow and iterated it consecutively to reduce the error, which is known as the *successive approximations* method. The generalized algorithm was responsible for providing the locations and sizes of the capacitor banks. Meanwhile, the optimal power flow method calculated the operating status of the system with the best configuration, minimizing the expected costs of energy losses. This methodology showed excellent results in several IEEE test feeders consisting of 33, 69, and 85 nodes.

Other algorithms employed for solving the mathematical model for the optimal integration of fixed-step capacitor banks in radial EDNs are the tabu search algorithm (19), the artificial bee colony optimizer (20), the particle swarm optimizer (21), modified genetic optimizers (22), and the cuckoo search optimizer (23), among others.

Although all of the aforementioned methods have shown excellent results, they all share the same problem: none of them ensures the best solution (global optimum) for the optimization model. This suggests that there may be better solutions. Additionally, they need to be calibrated, and, for this reason, their performance may vary among different testing systems. Furthermore, obtaining statistically reliable results requires multiple simulations. To address these issues, the study conducted by (14) proposed a conic programming model for mixed-integer (MI) optimization. This model ensures that an optimal solution to the optimization problem is obtained. However, this model was only evaluated in

test systems operating for an hour and did not consider the use of renewable energy sources, which can be impractical in today's world. Furthermore, this work neglected the stochastic aspects of renewable generators and the demand resulting from their uncertainties. Unlike the previous work, we present a stochastic MI convex model based on a branch flow optimization model. This model incorporates three different levels (*i.e.*, low, medium, and high) regarding the demand and generation by renewable energy sources, aiming to address the stochastic nature of EDNs by considering multiple operating conditions. The contributions of this study are listed below.

i. A stochastic mixed-integer branch flow (SMIBF) model is presented for the optimal integration (siting and sizing) of fixed-step capacitor banks in EDNs. The proposed SMIBF model incorporates three operating conditions for demand and generation: low, medium, and high levels. These conditions result in a total of nine scenarios.

ii. The proposed SMIBF model aims to minimize two objectives: the annual costs of energy losses and the costs of installing capacitor banks. These two objectives imply that the model is a multi-objective problem solved by incorporating a weighting factor.

iii. Three simulation scenarios are suggested to showcase the stochastic model's efficiency and compare it against three solvers accessible in the GAMS software.

The structure of this paper is as follows. Section 2 formulates the non-convex MINLP model to locate and size capacitor banks in EDNs. Section 3 formulates the proposed model using the branch flow optimization model. Section 4 outlines the three test feeders implemented and the load-generation scenarios considered. The primary findings and an analysis of the developed SMIBF model are presented in Section 5. Lastly, the main conclusions and proposals for future work are provided in Section 6.

2. Optimization model

The optimal integration (*i.e.*, placement and size) of fixed-step capacitor banks in EDNs enhances their operating conditions. These conditions are the reduction of congestion in distribution lines, the reduction of power losses, and the improvement of voltage profiles. This means that it is important to carefully select nodes for locating capacitor banks, as well as the banks' appropriate size, in order to avoid any negative impact on the operation of EDNs. This implies the need for a model aimed at optimally integrating capacitor banks in EDNs. In this vein, this model incorporates both continuous and binary variables. The continuous variables denote the nodal voltages, the power flows of the transmission lines, and the power generated by conventional generation and renewable energy sources, among others. Meanwhile, the binary variables only represent the location of the capacitor banks. The MINLP model for the problem under analysis is formulated below.

2.1. Optimization model objectives

The objective function (OF) z used for the optimal integration of capacitor banks in EDNs minimizes two parameters: the annual costs of energy losses (z_1) and the costs associated with capacitor bank installation (z_2). These two objectives indicate that the proposed model is a multi-objective problem

solved by incorporating a weighting factor (ω). The use of this factor is referred to as the *weighted sum method* (24), which turns the multi-objective problem into a single-objective one by assigning weights to each objective. Furthermore, the OF is normalized to adequately balance both objectives. Thus, the proposed OF takes the following form:

$$\text{mín } z = \omega \frac{z_1}{C_{\text{loss}}^{\text{máx}}} + (1 - \omega) \frac{z_2}{C_{\text{cap}}^{\text{máx}}} \tag{1}$$

$$z_1 = K_p \sum_{l \in \mathcal{B}} R_l i_l^2, \tag{2}$$

$$z_2 = \sum_{k \in \mathcal{N}} \sum_{t \in \mathcal{T}} K_t Q_t y_{kt}, \tag{3}$$

where $\omega \in [0, 1]$ represents the weighting factor, which assigns weight to each OF based on its value; K_p is a cost factor that quantifies the power losses, yielding the annual energy losses; R_l denotes the resistive effect of the transmission line connected to branch l; i_l is the magnitude of the current flowing through the transmission line connected to branch l; $\mathcal{B}$ and $\mathcal{N}$ correspond to the sets of the branches (or lines) and nodes in the distribution network, while $\mathcal{T}$ represents the set of capacitor bank types; K_t denotes the cost factor of the capacitor banks per kvar-year; Q_t is the nominal power of the capacitor bank type t; y_{kt} is the binary variable associated with the type or capacity of capacitor bank t and the connected node k; $C_{\text{loss}}^{\text{máx}}$ represents the cost of z_1 in the distribution grid without capacitor banks; and $C_{\text{cap}}^{\text{máx}}$ denotes the maximum possible costs related to the installation of these banks.

It is important to note that there are several approaches to solving multi-objective optimization problems, which can be broadly categorized into classical and evolutionary techniques, such as goal programming (25), Pareto-based methods (26), the weighted sum method (24), particle swarm optimization (27), genetic algorithms (27), differential evolution algorithms (27), the non-dominated sorting genetic algorithm II (NSGA-II) (28), the multi-objective evolutionary algorithm based on decomposition (29), and hybrid approaches. Although there are multiple methods to solve multi-objective problems, the weighted sum method was selected because it offers several advantages. These include conceptual simplicity, ease of implementation, flexibility in expressing preferences, the ability to transform the problem into a linear programming one, a unique approach, and the clear interpretation of solutions (30). However, it is also important to mention that this method has limitations and may not be suitable for all multi-objective problems, particularly those with non-convex Pareto fronts or highly non-linear problems.

2.2. Optimization model constraints

The set of model constraints for the optimal integration of fixed-step capacitor banks in EDNs is represented by the nodal power balance equations, the voltage drop in each branch, the maximum and minimum power capacity of the generators, the maximum and minimum voltage limits, and the number and size of the capacitor banks to be installed.

The nodal power balance equations are calculated so that the total power injected (or consumed) at each node is equivalent to the sum of the sending and receiving power flows through the branches

connected to it. The nodal power balance in each node can be formulated as follows:

$$A_k(P_l - R_l i_l^2) = p_{k,dg} - p_{k,d} \ \{k \in \mathcal{N}, \}, \tag{4}$$

$$A_k(Q_l - X_l i_l^2) = Q_{k,t} - q_{k,d} \ \{k \in \mathcal{N}\}, \tag{5}$$

where A_k in the incident matrix for node k (node-to-branch); P_l and Q_l are vectors that contain the active and reactive power flows of the branches, respectively; $p_{k,dg}$ is the active power generated via renewable energy sources at node k; $p_{k,d}$ and $q_{k,d}$ are the active and reactive power consumption at node k; $Q_{k,c}$ is the reactive power delivered by the capacitor bank connected to node k; and X_l is the reactance associated with branch l.

The voltage drop equation establishes a connection between the voltage and current at both ends of each branch while considering its resistance and reactance. The voltage loss in each branch can be formulated as follows:

$$v_m^2 = v_k^2 - 2\left(R_l p_l + X_l q_l\right) + \left(R_l^2 + X_l^2\right) i_l^2 \ \{l \in \mathcal{B}\}, \tag{6}$$

where v_m (or v_k) represents the magnitude of the voltage at node m (or k), p_l denotes the active power flow of branch l, and q_l is the reactive power flow of branch l.

The squared magnitude of the apparent power flowing through the branches can be defined as

$$v_l^2 i_l^2 = p_l^2 + q_l^2 \ \{l \in \mathcal{B}\}. \tag{7}$$

The limits regarding the maximum and minimum power from renewable energy sources and the maximum and minimum voltage bounds can be defined as follows:

$$p^{\mathrm{mín}} \leq p_{k,dg} \leq p^{\mathrm{máx}} \ \{k \in \mathcal{N}\}, \tag{8}$$

$$v^{\mathrm{mín}} \leq v_k \leq v^{\mathrm{máx}} \ \{k \in \mathcal{N}\}, \tag{9}$$

where $p^{\mathrm{mín}}$ and $p^{\mathrm{máx}}$ denote the renewable energy sources' minimum and maximum power; and $v^{\mathrm{mín}}$ and $v^{\mathrm{máx}}$ are the minimum and maximum voltage limits, respectively.

Box constraint (8) bounds the minimum and maximum active power available from renewable energy sources, while box constraint (9) is dictated by regulatory limits for the adequate operation of EDNs. The typical values are between $\pm 5\,\%$ and $\pm 10\,\%$ (31).

The ideal incorporation of capacitor banks in EDNs can be split into two components. The first involves determining their appropriate placement within the system, while the second determines the right size. These difficulties are addressed by implementing the following constraints:

$$Q_{k,c} = \sum_{t \in \mathcal{T}} y_{kt} Q_t^{\mathrm{nom}} \ \{\forall k \in \mathcal{N}\}, \tag{10}$$

$$\sum_{k \in \mathcal{N}} \sum_{t \in \mathcal{T}} y_{kt} \leq N^{\mathrm{cap}}, \tag{11}$$

where Q_t^{nom} is the nominal power of capacitor bank type t, and N^{cap} is the maximum number of capacitor banks to be incorporated into the EDN.

2.3. Interpretation of the optimization model

The optimization model for the optimal integration (siting and sizing) of fixed-step capacitor banks in EDNs, which is described in Eqs. (1) to (11), includes continuous variables associated with the magnitudes and angles of the nodal voltages, as well as with the active power generated via renewable energy sources and the reactive power injected by the fixed-step capacitor banks. At the same time, this optimization model incorporates binary variables associated with the location of the fixed-step capacitor banks in the EDN. The objective functions (2) and (3) and the set of constraints from (4) to (11) generate an MINLP model that has the following aspects.

The objective function (1) represents the total annual operating costs of an EDN. It consists of two terms: the first one (z_1) denotes the annual costs of energy losses in the EDN, while the second one (z_2) represents the costs associated with the installation of fixed-step capacitor banks. Constraints (4) and (5) represent the nodal active and reactive power balance, respectively. The left side of these constraints represents the power flowing through the distribution lines that reach the node, taking the corresponding losses into account. The right side denotes the energy generated or demanded at the same node. Constraint (6) corresponds to the voltage drop, which is represented in terms of the magnitude of the current flowing through the distribution lines and their parameters. Constraint (7) represents the squared magnitude of the apparent power flowing through the distribution lines, while inequalities (8) and (9) define the maximum and minimum values for the active power generated by renewable energy sources and the nodal voltages, respectively. Constraint (10) denotes the reactive power injected by a fixed-step capacitor bank, while constraint (11) regulates the maximum number of capacitor banks that can be included in the EDN.

Remark. *The MINLP model described from (1) to (11) contains the convex and non-convex constraints, which are represented by (4), (5), (6), and (7). This set of constraints poses significant issues in solving the MINLP model and ensuring its global optimum since, mathematically, it is not possible to demonstrate it. This means that the solution found by some methods is most likely a local optimum. Thereupon, the next section reformulates these constraints in order to transform them into a convex model and thus ensure the global optimum of the model.*

3. Branch flow reformulation

Auxiliary variables are defined which will be used to transform the non-convex MINLP optimization model into a convex one. These auxiliary variables are

$$V_k = v_k^2 \ \{k \in \mathcal{N}\}, \tag{12}$$

$$I_l = i_l^2 \ \{l \in \mathcal{B}\}. \tag{13}$$

Now, substituting these variables into Eqs. (4), (5), (6), and (7) yields the following:

$$A_k(P_{l,t} - R_l I_l) = p_{k,dg} - p_{k,d} \ \{k \in \mathcal{N},\}, \tag{14}$$

$$A_k(Q_{l,t} - X_l I_l) = Q_{k,c} - q_{k,d} \ \{k \in \mathcal{N}\}, \tag{15}$$

$$V_m = V_k - 2\left(R_l p_l + X_l q_l\right) + \left(R_l^2 + X_l^2\right) I_l \ \{l \in \mathcal{B}\}, \tag{16}$$

$$V_l I_l = p_l^2 + q_l^2 \ \{l \in \mathcal{B}\}. \tag{17}$$

Note that the constraints (14), (15), and (16) are linear expressions, and thus they are convex constraints. Nevertheless, the constraints in (17) continue to be a non-convex due to the product between the auxiliary variables. This product can be rewritten as follows:

$$
\begin{aligned}
v_l^2 i_l^2 &= \frac{1}{4}\left(I_l + V_k\right)^2 - \frac{1}{4}\left(I_l - V_k\right)^2 = p_l^2 + q_l^2 \\
\frac{1}{4}\left(I_l + V_k\right)^2 &= p_l^2 + q_l^2 + \frac{1}{4}\left(I_l - V_k\right)^2 \\
\left(I_l + V_k\right)^2 &= 4p_l^2 + 4q_l^2 + \left(I_l - V_k\right)^2 \\
I_l + V_k &= \sqrt{4p_l^2 + 4q_l^2 + \left(I_l - V_k\right)^2}.
\end{aligned}
\tag{18}
$$

The constraint (18) can be expressed using norm-2, as follows:

$$
I_l + V_k = \left\| \begin{array}{c} 2p_l \\ 2q_l \\ I_l - V_k \end{array} \right\|.
\tag{19}
$$

Note that the constraint (18) is still a non-convex expression, even though it has been transformed into a second-order conic constraint. However, it can be made convex by relaxing the equality to an inequality, as demonstrated in (32). The convex formulation of the second-order conic constraint takes the following form:

$$
I_l + V_k \geq \left\| \begin{array}{c} 2p_l \\ 2q_l \\ I_l - V_k \end{array} \right\|.
\tag{20}
$$

The convex model for the optimal integration of fixed-step capacitor banks in EDNs is as follows:

$$
\text{mín } z = \omega \frac{z_1}{C_{\text{loss}}^{\text{máx}}} + (1-\omega)\frac{z_2}{C_{\text{cap}}^{\text{máx}}}
\tag{21}
$$

$$
z_1 = K_p \sum_{l \in \mathcal{B}} R_l I_l,
\tag{22}
$$

$$
z_2 = \sum_{k \in \mathcal{N}} \sum_{t \in \mathcal{T}} K_t Q_t y_{kt},
\tag{23}
$$

Subject to:

$$
A_k(P_{l,t} - R_l I_l) = p_{k,dg} - p_{k,d} \ \{k \in \mathcal{N}, \},
\tag{24}
$$

$$
A_k(Q_{l,t} - X_l I_l) = Q_{k,c} - q_{k,d} \ \{k \in \mathcal{N}\},
\tag{25}
$$

$$
V_m = V_k - 2\left(R_l p_l + X_l q_l\right) + \left(R_l^2 + X_l^2\right) I_l \ \{l \in \mathcal{B}\},
\tag{26}
$$

$$
I_l + V_k \geq \left\| \begin{array}{c} 2p_l \\ 2q_l \\ I_l - V_k \end{array} \right\| \ \{l \in \mathcal{B}, \ k \in \mathcal{N}\},
\tag{27}
$$

$$p^{\text{mín}} \leq p_{k,dg} \leq p^{\text{máx}} \ \{k \in \mathcal{N}\}, \tag{28}$$

$$v^{\text{mín}} \leq v_k \leq v^{\text{máx}} \ \{k \in \mathcal{N}\}, \tag{29}$$

$$Q_{k,c} = \sum_{t \in \mathcal{T}} y_t Q_t^{\text{nom}} \ \{\forall k \in \mathcal{N}\}, \tag{30}$$

$$\sum_{k \in \mathcal{N}} \sum_{t \in \mathcal{T}} y_{kt} \leq N^{\text{cap}}. \tag{31}$$

The main benefit of the mixed-integer branch flow model, as outlined from (21) to (31), is its ability to find the global optimum. A combination of the cutting plane algorithm and the interior point method can be used to find the solution to this optimization model. However, it is essential to note that this model does not consider the stochastic nature of demand and renewable energy sources, which will be included in the following subsection.

3.1. Stochastic MI branch flow model

An EDN experiences various operating conditions as a result of fluctuating generation from renewable energy sources and changing demand. Hence, it is crucial to establish a minimum number of potential scenarios for the problem under study. In this context, the OF value (21) can be expressed as the sum of each scenario considered, multiplied by the probability of occurrence. This approach is known as the *sample average approximation model* (33) and is defined as follows:

$$\text{mín } \Xi(z_1, z_2, \xi_s) = \sum_{s \in \mathcal{S}} \xi_s z, \tag{32}$$

where ζ_s is the probability factor of occurrence for scenario s, and $\mathcal{S}$ represents the set of scenarios.

Remark. *Note that the OF* (32) *remains linear (an affine function). As a result, it is convex, and its global optimum can be ensured. Nevertheless, it is crucial to limit the amount of scenarios in order to make the optimization model more manageable.*

The proposed SMIBF model is formulated below.

$$\text{mín } \sum_{s \in \mathcal{S}} \xi_z z$$
$$\text{Subject to: } (21) - (31). \tag{33}$$

4. Test system under study

The proposed SMIBF model was tested through numerical experiments on three modified, well-known distribution networks, *i.e.*, the 33-, 69-, and 85-node test feeders. For the sake of simplicity, these test systems will be referred to as *Test Feeder 1*, *Test Feeder 2*, and *Test Feeder 3*, respectively. The renewable energy sources considered are photovoltaic (PV) power plants, and three of them are incorporated in each test feeder. The main features of each test feeder are outlined below.

4.1. Test Feeder 1

Test Feeder 1 is a radial EDN, with 32 transmission lines and 33 nodes. It operates at 12,66 kV at the slack node (bus 1) and has a peak apparent power demand of $3,715$ kW $+ j2,300$ kvar. For this peak demand, the test feeder experiences apparent power losses of approximately $210,9876$ kW $+ j143,1283$ kvar. The three PV power plants are located at buses 13, 24, and 30, and their rated powers are 801,8, 1.091,3, and 1.053,6 kW, respectively. These locations and sizes were taken from (34). Fig. **1** illustrates the topology of Test Feeder 1 with three PV power plants. This grid considers 12,66 kV and 1 MW as its voltage and power bases. The main information about this test feeder can be consulted in (35).
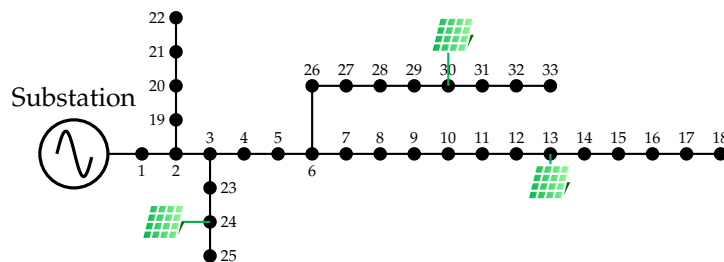

Figure 1. Topology of Test Feeder 1 with three PV power plants

4.2. Test Feeder 2

Test Feeder 2 has a radial configuration, 68 transmission lines, and 69 nodes. It operates at a voltage of 12,66 kV at the slack node (bus 1), and its peak apparent power demand is $3,890,7$ kW$+j2,693,6$ kvar. The apparent power losses of this peak demand are approximately $224,9520$kW $+ j102,3559$ kvar. In this test feeder, the locations of the PV power plant are at buses 11, 18, and 61, with nominal powers of 1.631,31, 463,33, and 503,80 kW, respectively. This information has been taken from (34). Fig. **2** depicts the topology of Test Feeder 2 and the three PV power plants. The base values used for power and voltage are 1 MW and 12,66 kV. The main information about this test feeder can consulted in (35).
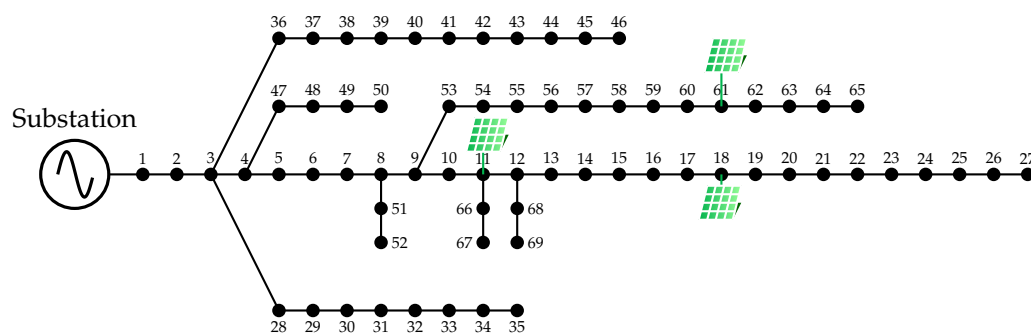

Figure 2. Topology of Test Feeder 2 with three PV power plants

4.3.   Test Feeder 3

Test Feeder 3 has a radial topology, with 84 transmission lines and 85 nodes. It operates at a rated voltage of 11 kV at the slack node (bus 1) and has a peak apparent power demand of $2,570,28$ kW $+ j2,622,20$ kvar. The nominal powers of the three PV power plants are 526,8, 380,1, and 1.719 kW, and they are located at nodes 35, 67, and 71, respectively. This information can be consulted in (36). Fig. **3** shows the topology of Test Feeder 3. This system considers 11 kV and 1 MW as its voltage and power bases.
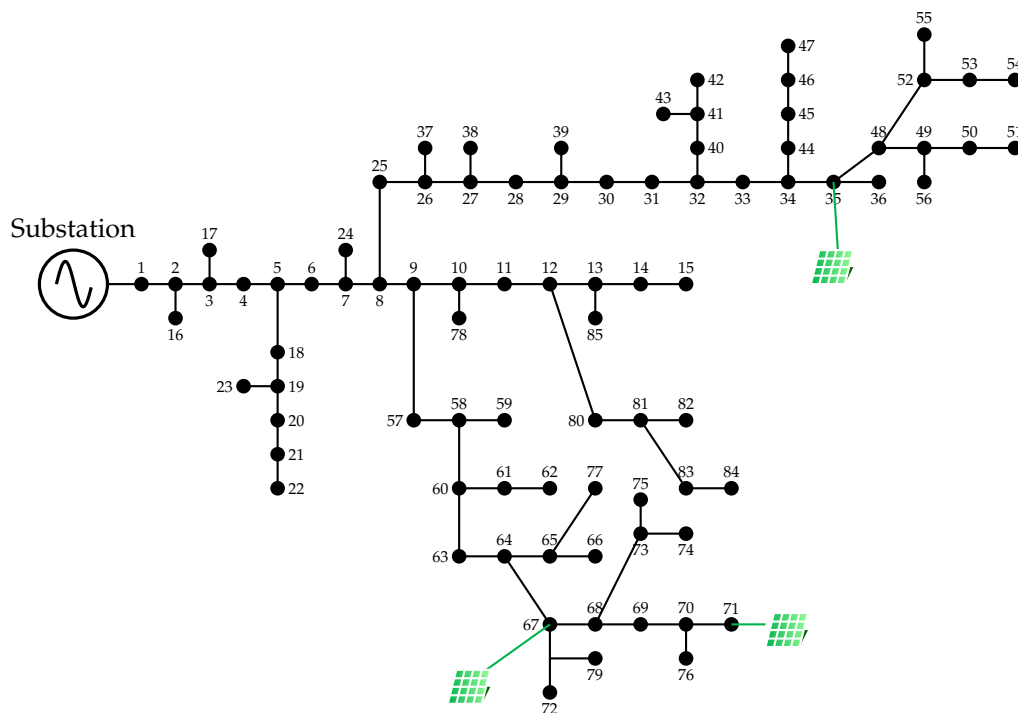

Figure 3. Topology of Test Feeder 3 with three PV power plants

4.4.   Load-generation scenario

The number of scenarios plays a crucial role in analyzing uncertain situations; a reliable and manageable model must have an adequate number of scenarios. This research examines three distinct scenarios related to PV power plant generation and demand conditions. These scenarios incorporate low, medium, and high levels, resulting in nine potential combinations of renewable energy generation and load consumption, each with its own probability. The accuracy of the optimization model could be enhanced by increasing the number of scenarios. However, this would generate a large computational effort with little potential benefit. The probability factor used in this paper for each scenario can be consulted in (37).

The cost coefficient K_p used is equal to 168 US$/kW-year, and the capacitor bank data for the optimization model are shown in Table **I**. This information was taken from (14).

Table I. Size and costs per capacitor bank

Type	Q_t (kvar)	**Cost** (USD\$/kvar-year)	Type	Q_t (kvar)	**Cost** (USD\$/kvar-year)
1	150	0,500	8	1.200	0,170
2	300	0,350	9	1.350	0,207
3	450	0,253	10	1.500	0,201
4	600	0,220	11	1.650	0,193
5	750	0,276	12	1.800	0,870
6	900	0,183	13	1.950	0,211
7	1.050	0,228	14	2.100	0,176

5. Numerical results and discussions

The SMIBF model was executed in the CVX interface, which allows modeling convex optimization problems in MATLAB (38). The solver used in CVX was Gurobi. Additionally, the non-convex MINLP model was implemented in GAMS and solved by employing the BONMIN, KNITRO, and DICOPT solvers. Three simulation cases were proposed to evaluate the effectiveness of the SMIBF model:

C1 This case assumes that only three capacitor banks can be installed.

C2 This case analyzes the effect on the OF z with varying numbers of capacitor banks on the systems. It considers a range of 0-5.

C3 This case generates a Pareto front by varying the weighting factor between 0 and 1. This case only considers the installation of three capacitor banks.

5.1. Results obtained for C1

This case evaluates the efficiency of the SMIBF model and compares it against the non-convex model solved in GAMS using three different solvers. Table **II** presents the results obtained regarding the OF value in Eq. (33), its reduction compared to the benchmark case, and the reduction of power losses. The cost factors $C_{\mathrm{loss}}^{\mathrm{máx}}$ for Test Feeders 1, 2, and 3 are USD 9.010,848, USD 11.422,13, and USD 14.846,52, respectively. Moreover, $C_{\mathrm{cap}}^{\mathrm{máx}} = \mathrm{USD}4{,}698$.

According to results shown in Table **II**, it can be stated that:

- The best solution was found by the proposed SMIBF model in the three test feeders. The OF values for these feeders are 0,6019, 0,6521, and 0,44769, which have been recalculated from the non-convex MINLP model. Regarding the benchmark cases, there were reductions of 39,81, 35,29, and 56,31 % in Test Feeders 1, 2, and 3, respectively, when compared to the best solutions. The reductions in energy losses are approximately 46,44, 40,39, and 63,77 %, respectively.

- As for Test Feeder 1, it is worth noting that the BONMIN solver achieved a solution close to that of the proposed SMIBF formulation. However, this solution is a local optimum that reduces the

Table II. Optimal integration of capacitor banks for case C1

Method	Nodes	Size (kvar)	Objective function	Reduction (%)	Reduction loss (%)
			Test Feeder 1		
Benchmark case			1	–	–
BONMIN	{8,14,30}	{150,150,600}	0,6068	39,32	45,3182
KNITRO	{7,25,30}	{900,150,450}	0,6631	33,69	41,2092
DICOPT	{7,24,25}	{900,150,150}	0,7406	25,94	32,6318
SMIBF	{12,25,30}	{300,150,600}	0,6019	39,81	46,4446
			Test Feeder 2		
Benchmark case			1	–	–
BONMIN	{11,61,64}	{900,900,150}	0,7884	21,16	29,7676
DICOPT	{25,50,61}	{150,150,600}	0,6619	33,81	40,4994
SMIBF	{21,61,64}	{150,600,150}	0,6471	35,29	40,3941
			Test Feeder 3		
Benchmark case			1	–	–
SMIBF	{9,34,68}	{600,450,300}	0,4369	56,31	63,7771

OF and energy losses by 39,32 and 45,3182 %, respectively. On the other hand, the KNITRO and DICOPT solvers obtained the worst solutions, reducing the OF value by 33,69 and 25,94 %.

- In the case of Test Feeder 2, the KNITRO solver had convergence problems and was unable to find a feasible solution. Meanwhile, the BONMIN solver yielded the worst solution overall; it only minimally reduced the OF value by 21,16$. On the contrary, the DICOPT solver found a solution close to that of the proposed SMIBF formulation, reducing the OF value by 33.81 %. Note that, regarding Test Feeder 3, none of the solvers could converge to any feasible solution, which is why this information is not included in Table **II**.

- These results demonstrate that the non-convex MINLP model for the optimal integration of fixed-step capacitor banks in EDNs is a challenging problem to solve. No solver in GAMS was able to find the best configuration. Additionally, as the test systems increase in size, the solvers encounter convergence problems. This shows that a convex formulation is better for solving this type of optimization model, even if it is relaxed.

Fig. **4** compares the average voltage profiles of the test systems, considering the presence or absence of capacitor banks. Based on this figure, it can be argued that, when capacitor banks are incorporated into the EDNs, the average voltage profiles are improved, *i.e.*, they remain closer to 1,0 pu. In Figure **4**a, the worst average voltage profile, with or without capacitor banks installed, corresponds to node 18. However, it increases from 0,9804 to 0,9650 pu, *i.e.*, an improvement of approximately 1,60 %. For Test Feeder 2, the worst average voltage profiles (Fig. **4**b) are 0,968 and 0,9560 pu (both at node 65) with and without capacitor banks installed. The improvement was around 1,28 %. In the case of Test Feeder 3, the improvement was around 2,91 %, going from a voltage level of 0,9464 pu (without capacitor banks) to 0,9740 pu (with capacitor banks) at node 54 (Fig. **4**c). Additionally, in Figs. **4**b and **4**c, it can be noted that all voltages are above the minimum limit ($\geq 0,95$ pu) when the capacitor banks are installed, as opposed to not having them in the systems.
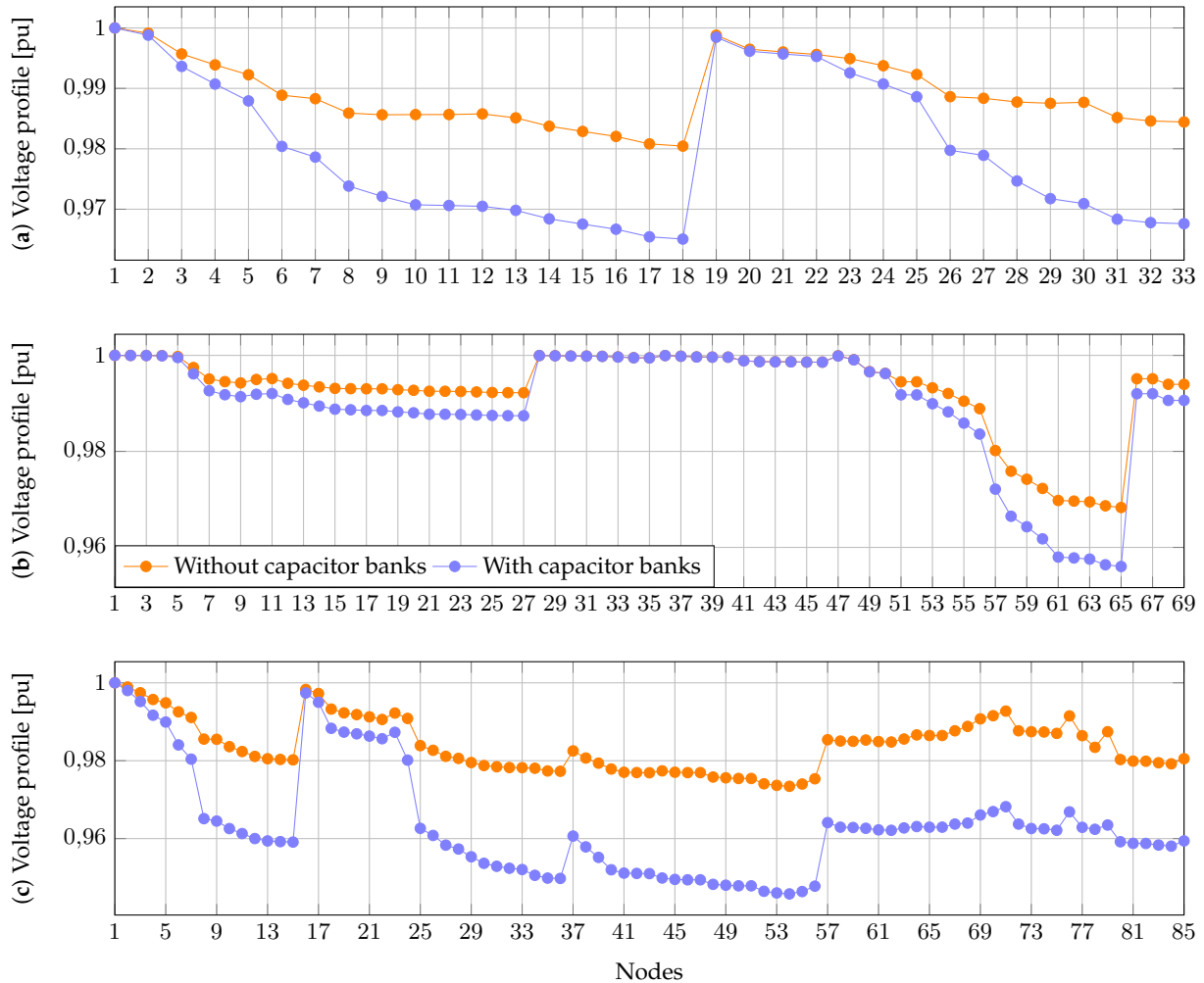
Figure 4. Comparison of average voltage profiles with and without capacitor banks installed: a) Test Feeder 1, b) Test Feeder 2, and c) Test Feeder 3

5.2. Results obtained for C2

This case analyzed how the OF is affected by changing the amount of capacitor banks installed from 0 to 5. Fig. **5** displays the value of the OF in (33) as the amount of capacitor banks increases in the three test feeders.

The results presented in Fig. **5** show that the addition of a third bank of capacitors does not lead to any improvements in the OF value; in fact, it makes it worse. This indicates that there is no significant reduction in system power losses after the third bank of capacitors – note that the installation of the capacitors increases the costs. For Test Feeder 2, the OF value is not significantly improved after installing the first capacitor bank. This improvement is reduced from having just one to three banks by only 0,35 %. A similar situation occurs for Test Feeders 1 and 3: the OF is reduced by 0,30 and 1,64 %, respectively, when going from two to three banks.
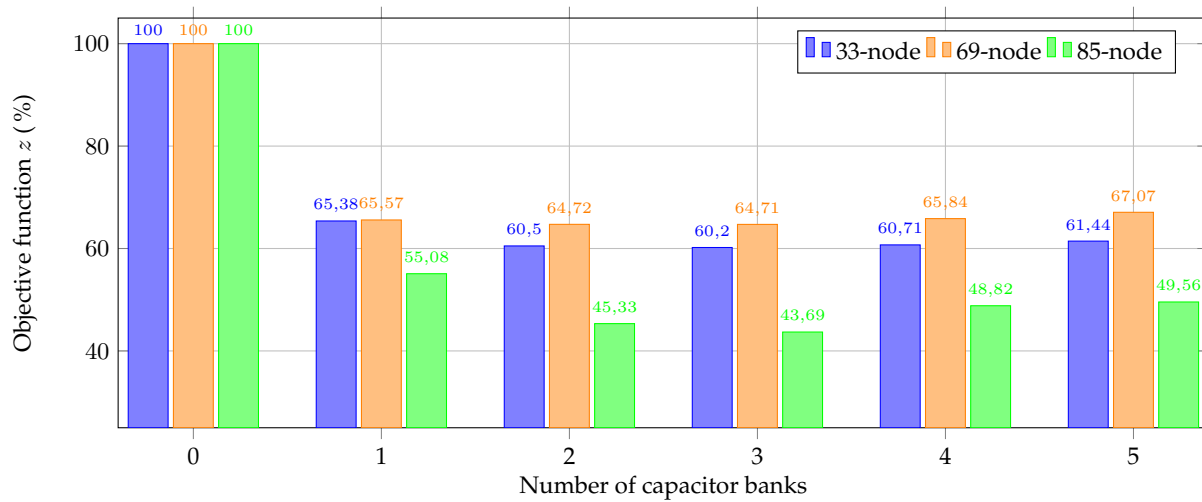
Figure 5. Variations in the objective function value with respect to the number of capacitor banks

5.3. Results obtained for C3

This case analyzes the Pareto set by increasing the ω factor by 0,1 from 0 to 1 in the OF z described in (21). Table **III** presents the OF values for all test feeders, which have been calculated via the SMIBF model.

Table III. Pareto data regarding the objective functions for the proposed SMIBF model

	z	z_1	z_2	z	z_1	z_2	z	z_1	z_2
Factor (ω)	Test Feeder 1			69-node test feeder			Test Feeder 3		
0,0	1	1	0	1	1	0	1	1	0
0,1	0,6601	0,6320	0,0280	0,6761	0,6480	0,0280	0,6078	0,5797	0,0280
0,2	0,6601	0,6320	0,0280	0,6761	0,6480	0,0280	0,4573	0,3971	0,0561
0,3	0,6050	0,5545	0,0504	0,6761	0,6480	0,0280	0,4573	0,3971	0,0561
0,4	0,6050	0,5545	0,0504	0,6471	0,5961	0,0510	0,4387	0,3660	0,0727
0,5	0,6019	0,5355	0,0664	0,6471	0,5961	0,0510	0,4369	0,3622	0,0746
0,6	0,6031	0,5303	0,0727	0,6471	0,5961	0,0510	0,4369	0,3622	0,0746
0,7	0,6031	0,5303	0,0727	0,6601	0,5841	0,0759	0,4369	0,3622	0,0746
0,8	0,6031	0,5303	0,0727	0,6601	0,5841	0,0759	0,4552	0,3664	0,0887
0,9	0,6031	0,5303	0,0727	0,6654	0,5830	0,0823	0,4552	0,3664	0,0887
1,0	0,6031	0,5303	0,0727	0,6654	0,5830	0,0823	0,4552	0,3664	0,0887

From the Pareto set results in Table **III**, it is possible to conclude that:

- Both objective functions, z_1 and z_2, are in conflict because, as the value of the first one decreases (improves), that of the second one increases (deteriorates). The extreme solutions occur at the minimum and maximum values of the weighting factor, *i.e.*, when $\omega = 0$ and $\omega = 1$. The maximum weighting factor solution reveals that the annual energy losses costs for Test Feeders 1, 2, and 3 are

USD 9.010,848, 11.422,13, and USD 14.846,52, respectively. An analysis of the minimum weighting factor reveals that the investment costs for installing capacitor banks are highest at USD 341,5446, 386,6454, and 416,7126 per year for the modified Test Feeders 1, 2, and 3, respectively. However, in this solution, the annual energy losses costs are the lowest for the three test systems.

- The optimal solution of the OF z (*i.e.*, the multi-objective scenario) was found for $\omega = 0,5$ in each test feeder. This shows that the weighting factor for the single-objective scenario does not substantially impact the final result of the proposed SMIBF model. Nevertheless, the benefit of the Pareto set lies in having a spectrum of solutions that energy companies can use to make better decisions for their electrical systems.

5.4. Discussing the influence of integrating energy storage systems and the effect of radial reconfiguration on the model

In modern distribution systems, the integration of energy storage systems (ESS) introduces a dynamic element that could influence the optimal location and sizing of capacitors. The presence of ESS alters the overall energy flow patterns and affects the voltage profile across the grid. When incorporating fixed-step capacitor banks, co-optimization with storage systems becomes crucial. Storage systems can help alleviate the intermittency of renewable energy sources, which affects the requirements for reactive power compensation. The optimal placement of capacitors is intricately linked to the temporal and spatial dynamics of energy storage, as the latter influence load profiles and voltage stability. This dynamic interaction adds a layer of complexity to the model by introducing non-linearities caused by the time-dependent nature of storage systems (39). Consequently, the stochastic mixed-integer branch flow optimization model needs to evolve to capture these complex relationships, considering the dynamic nature of energy flow and voltage support in the presence of storage technologies.

On the other hand, the reconfiguration of electric distribution networks, particularly the transition to new radial configurations, could significantly influence the integration of fixed-step capacitors. Radial reconfiguration aims to enhance system reliability and minimize power losses by modifying the network's topology. In this context, the integration of fixed-step capacitors is a strategic endeavor. The new radial configurations may result in changes in load distribution and voltage profiles. To optimize the integration of capacitors, their location and size must be recalibrated to align with the new network conditions. Capacitors play a crucial role in compensating for reactive power demand and minimizing losses. Therefore, the strategic deployment of these devices is essential for achieving the objectives of the reconfigured network, such as minimizing losses and enhancing overall reliability. This is particularly important when considering altered power flow paths. Control strategies for capacitor banks may also need to be adapted in order to effectively address the dynamic changes introduced by radial reconfiguration (40).

6. Conclusions and future works

This paper proposes an SMIBF model to optimally integrate fixed-step capacitor banks into EDNs. The aim is to reduce the annual costs of energy losses and those of installing this technology. Our

proposal is based on a branch flow optimization model that incorporates two sets of auxiliary variables in order to generate a convex model and thus the global optimum. Furthermore, the model incorporates the sample average approximation model to address the stochastic nature of EDNs under multiple operating conditions. This allows for the inclusion of three different conditions into the developed model with regard to demand and renewable generation, namely low, medium, and high levels. The performance of the proposed model was evaluated on three test feeders and compared to the solutions provided by the BONMIN, KNITRO, and DICOPT solvers available in the GAMS software. The simulation results indicate that the developed SMIBF model provides the best solution for all three system, reducing the OF value by 39,81, 35,29, and 56,31 % in Test Feeders 1, 2, and 3 when compared to the benchmark case. At the same time, the annual energy losses were reduced by 46,44, 40,39, and 63,77 %, respectively. No GAMS solver was able to achieve the global optimum of the optimization model. Additionally, the solver exhibited convergence problems as the size of the test feeders increased. This demonstrates that our proposal is a better option for optimally integrating fixed-step capacitor banks, even though it corresponds to a relaxed model.

The impact of increasing the amount of capacitor banks on the OF value was analyzed, finding that, after adding three capacitor banks, the OF value becomes worse. This implies that the energy losses were not significantly reduced after three capacitor banks. On the other hand, the use of the weighting factor allowed implementing a multi-objective approach. When $\omega = 0,50$, this approach yields the best solution (minimum). This finding confirms that the developed SMIBF model successfully identifies the global optimum in every evaluation.

The following future works could be conducted: (i) considering fixed-step switched capacitor banks in the proposed model, (ii) simultaneously integrating fixed-step capacitor banks and D-FACTS devices, and (iii) extending the developed SMIBF model to large-scale transmission systems with new objective functions.

7. Acknowledgments

8. Author contributions

All authors contributed equally to the research.

References

[1] M. I. M. Ridzuan, N. F. M. Fauzi, N. N. R. Roslan, and N. M. Saad, "Urban and rural medium voltage networks reliability assessment," *SN Appl. Sci.*, vol. 2, no. 2, jan 2020. [Online]. Available:

https://doi.org/10.1007/s42452-019-1612-z ↑ 4

[2] L. C. Kien, T. T. Nguyen, T. D. Pham, and T. T. Nguyen, "Cost reduction for energy loss and capacitor investment in radial distribution networks applying novel algorithms," *Neural Comput. Appl.*, vol. 33, no. 22, pp. 15 495–15 522, jun 2021. [Online]. Available: SpringerScienceandBusinessMedia{LLC} ↑ 4

[3] A. Paz-Rodríguez, J. F. Castro-Ordoñez, O. D. Montoya, and D. A. Giral-Ramírez, "Optimal Integration of Photovoltaic Sources in Distribution Networks for Daily Energy Losses Minimization Using the Vortex Search Algorithm," *Appl. Sci.*, vol. 11, no. 10, p. 4418, may 2021. [Online]. Available: https://doi.org/10.3390/app11104418 ↑ 4

[4] A. Águila, L. Ortiz, R. Orizondo, and G. López, "Optimal location and dimensioning of capacitors in microgrids using a multicriteria decision algorithm," *Heliyon*, vol. 7, no. 9, p. e08061, sep 2021. [Online]. Available: https://doi.org/10.1016/j.heliyon.2021.e08061 ↑ 4

[5] E. P. Madruga and L. N. Canha, "Allocation and integrated configuration of capacitor banks and voltage regulators considering multi-objective variables in smart grid distribution system," in *2010 9th IEEE/IAS International Conference on Industry Applications - INDUSCON 2010*, 2010, pp. 1–6. [Online]. Available: https://doi.org/10.1109/INDUSCON.2010.5740055 ↑ 4

[6] L. A. G. Pareja, J. M. L. Lezama, and O. G. Carmona, "Optimal placement of capacitors, voltage regulators, and distributed generators in electric power distribution systems," *Ingeniería*, vol. 25, no. 3, pp. 334–354, oct 2020. [Online]. Available: https://doi.org/10.14483/23448393.16925 ↑ 4

[7] S. Mishra, D. Das, and S. Paul, "A comprehensive review on power distribution network reconfiguration," *Energy Syst.*, vol. 8, no. 2, pp. 227–284, mar 2016. [Online]. Available: https://doi.org/10.1007/s12667-016-0195-7 ↑ 4

[8] S. Dhivya and R. Arul, "Demand side management studies on distributed energy resources: A survey," *TESEA Trans.*, vol. 2, no. 1, pp. 17–31, jul 2021. [Online]. Available: https://doi.org/10.32397/tesea.vol2.n1.2 ↑ 4

[9] R. Sirjani and A. R. Jordehi, "Optimal placement and sizing of distribution static compensator (D-STATCOM) in electric distribution networks: A review," *Renew. Sust. Energ. Rev.*, vol. 77, pp. 688–694, sep 2017. [Online]. Available: https://doi.org/10.1016/j.rser.2017.04.035 ↑ 4

[10] V. Tamilselvan, T. Jayabarathi, T. Raghunathan, and X.-S. Yang, "Optimal capacitor placement in radial distribution systems using flower pollination algorithm," *Alex. Eng. J.*, vol. 57, no. 4, pp. 2775–2786, dec 2018. [Online]. Available: https://doi.org/10.1016/j.aej.2018.01.004 ↑ 4

[11] A. Valencia, R. A. Hincapie, and R. A. Gallego, "Optimal location, selection, and operation of battery energy storage systems and renewable distributed generation in medium-low voltage distribution networks," *J. Energy Storage*, vol. 34, p. 102158, feb 2021. [Online]. Available: https://doi.org/10.1016/j.est.2020.102158 ↑ 4

[12] S. Griot and A. Moreau, "Vacuum circuit breaker's electrical life for shunt capacitor switching," in *24th ISDEIV 2010*, 2010, pp. 194–197. [Online]. Available: https://doi.org/10.1109/DEIV.2010.5625750 ↑ 4

[13] R. M. A. Velásquez and J. V. M. Lara, "Reliability, availability and maintainability study for failure analysis in series capacitor bank," *Eng. Fail. Anal.*, vol. 86, pp. 158–167, apr 2018. [Online]. Available: https://doi.org/10.1016/j.engfailanal.2018.01.008 ↑4

[14] O. D. Montoya, W. Gil-González, and A. Garcés, "On the conic convex approximation to locate and size fixed-step capacitor banks in distribution networks," *Computation*, vol. 10, no. 2, p. 32, 2022. [Online]. Available: https://doi.org/10.3390/computation10020032

[15] W. Gil-González, O. D. Montoya, A. Rajagopalan, L. F. Grisales-Noreña, and J. C. Hernández, "Optimal selection and location of fixed-step capacitor banks in distribution networks using a discrete version of the vortex search algorithm," *Energies*, vol. 13, no. 18, p. 4914, sep 2020. [Online]. Available: https://doi.org/10.3390/en13184914 ↑5

[16] F. E. Riaño, J. F. Cruz, O. D. Montoya, H. R. Chamorro, and L. Alvarado-Barrios, "Reduction of losses and operating costs in distribution networks using a genetic algorithm and mathematical optimization," *Electronics*, vol. 10, no. 4, p. 419, feb 2021. [Online]. Available: https://doi.org/10.3390/electronics10040419 ↑5

[17] I. P. Abril, "Capacitors placement in distribution systems with nonlinear load by using the variables' inclusion and interchange algorithm," *DYNA*, vol. 88, no. 217, pp. 13–22, may 2021. [Online]. Available: https://doi.org/10.15446/dyna.v88n217.91145 ↑5

[18] O. D. Montoya, W. Gil-González, and J. C. Hernández, "Efficient integration of fixed-step capacitor banks and D-STATCOMs in radial and meshed distribution networks considering daily operation curves," *Energies*, vol. 16, no. 8, p. 3532, 2023. [Online]. Available: https://doi.org/10.3390/en16083532 ↑5

[19] Y. Ogita and H. Mori, "Parallel dual tabu search for capacitor placement in smart grids," *Procedia Comput. Sci.*, vol. 12, pp. 307–313, 2012. [Online]. Available: https://doi.org/10.1016/j.procs.2012.09.076 ↑5

[20] A. A. El-Fergany and A. Y. Abdelaziz, "Capacitor placement for net saving maximization and system stability enhancement in distribution networks using artificial bee colony-based approach," *Int. J. Electr. Power Energy Syst.*, vol. 54, pp. 235–243, 2014. [Online]. Available: https://doi.org/10.1016/j.ijepes.2013.07.015 ↑5

[21] K. Prakash and M. Sydulu, "Particle swarm optimization based capacitor placement on radial distribution systems," in *2007 IEEE Power Engineering Society General Meeting*, 2007, pp. 1–5. [Online]. Available: https://doi.org/10.1109/PES.2007.386149 ↑5

[22] A. Augugliaro, L. Dusonchet, S. Favuzza, M. G. Ippolito, S. Mangione, and E. R. Sanseverino, "A modified genetic algorithm for optimal allocation of capacitor banks in MV distribution networks," *Intell. Ind. Syst.*, vol. 1, no. 3, pp. 201–212, sep 2015. [Online]. Available: https://doi.org/10.1007/s40903-015-0019-4 ↑5

[23] K. Devabalaji, T. Yuvaraj, and K. Ravi, "An efficient method for solving the optimal sitting and sizing problem of capacitor banks based on cuckoo search algorithm," *Ain Shams Eng. J.*, vol. 9, no. 4, pp. 589–597, dec 2018. [Online]. Available: https://doi.org/10.1016/j.asej.2016.04.005 ↑5

[24] R. T. Marler and J. S. Arora, "The weighted sum method for multi-objective optimization: new insights," *Struct. Multidiscipl. Optim.*, vol. 41, pp. 853–862, 2010. [Online]. Available: https://doi.org/10.1007/s00158-009-0460-7 ↑7

[25] D. Jones, M. Tamiz *et al.*, *Practical goal programming*.   Springer, 2010, vol. 141. [Online]. Available: https://doi.org/10.1007/978-1-4419-5771-9 ↑ 7

[26] S. Dutta and K. N. Das, "A survey on pareto-based eas to solve multi-objective optimization problems," in *Soft Computing for Problem Solving*.   Springer Singapore, 2019, pp. 807–820. [Online]. Available: https://doi.org/10.1007/978-981-13-1595-4_64 ↑ 7

[27] M. T. Emmerich and A. H. Deutz, "A tutorial on multiobjective optimization: fundamentals and evolutionary methods," *Nat. Comput.*, vol. 17, pp. 585–609, 2018. [Online]. Available: https://doi.org/10.1007/s11047-018-9685-y ↑ 7

[28] L. Zhihuan, L. Yinhong, and D. Xianzhong, "Non-dominated sorting genetic algorithm-ii for robust multi-objective optimal reactive power dispatch," *IET Gener. Transm. Distrib.*, vol. 4, no. 9, pp. 1000–1008, 2010. [Online]. Available: https://doi.org/10.1049/iet-gtd.2010.0105 ↑ 7

[29] S. Özdemir, B. A. Attea, and Ö. A. Khalil, "Multi-objective evolutionary algorithm based on decomposition for energy efficient coverage in wireless sensor networks," *Wirel. Pers. Commun.*, vol. 71, pp. 195–215, 2013. [Online]. Available: https://doi.org/10.1007/s11277-012-0811-3 ↑ 7

[30] J. B. Chagas and M. Wagner, "A weighted-sum method for solving the bi-objective traveling thief problem," *Comput Oper Res*, vol. 138, p. 105560, 2022. [Online]. Available: https://doi.org/10.1016/j.cor.2021.105560 ↑ 7

[31] P. Yu, C. Wan, M. Sun, Y. Zhou, and Y. Song, "Distributed voltage control of active distribution networks with global sensitivity," *IEEE Trans. Power Syst.*, vol. 37, no. 6, pp. 4214–4228, 2022. [Online]. Available: https://doi.org/10.1109/TPWRS.2022.3153954 ↑ 8

[32] M. Farivar and S. H. Low, "Branch flow model: relaxations and convexification—part i," *IEEE Trans. Power Syst.*, vol. 28, no. 3, pp. 2554–2564, aug 2013. [Online]. Available: https://doi.org/10.1109/tpwrs.2013.2255317 ↑ 10

[33] B. Verweij, S. Ahmed, A. J. Kleywegt, G. Nemhauser, and A. Shapiro, "The sample average approximation method applied to stochastic routing problems: a computational study," *Comput Optim Appl*, vol. 24, pp. 289–333, 2003. [Online]. Available: https://doi.org/10.1023/A:1021814225969 ↑ 11

[34] W. Gil-González, A. Garces, O. D. Montoya, and J. C. Hernández, "A mixed-integer convex model for the optimal placement and sizing of distributed generators in power distribution networks," *Appl. Sci.*, vol. 11, no. 2, p. 627, 2021. [Online]. Available: https://doi.org/10.3390/app11020627 ↑ 12

[35] O. D. Montoya, W. Gil-González, and L. Grisales-Noreña, "An exact MINLP model for optimal location and sizing of DGs in distribution networks: A general algebraic modeling system approach," *Ain Shams Eng. J.*, vol. 11, no. 2, pp. 409–418, 2020. [Online]. Available: https://doi.org/10.1016/j.asej.2019.08.011 ↑ 12

[36] O. D. Montoya, L. F. Grisales-Noreña, L. Alvarado-Barrios, A. Arias-Londoño, and C. Álvarez-Arroyo, "Efficient reduction in the annual investment costs in AC distribution networks via optimal integration of solar PV sources using the newton metaheuristic algorithm," *Appl. Sci.*, vol. 11, no. 23, p. 11525, 2021. [Online]. Available: https://doi.org/10.3390/app112311525 ↑ 13

[37] W. Gil-González, "Optimal placement and sizing of d-statcoms in electrical distribution networks using a stochastic mixed-integer convex model," *Electronics*, vol. 12, no. 7, p. 1565, 2023. [Online]. Available: https://doi.org/10.3390/electronics12071565 ↑ 13

[38] M. Grant and S. Boyd, "CVX: Matlab software for disciplined convex programming, version 2.1," mar 2014. [Online]. Available: http://cvxr.com/ ↑ 14

[39] H. A. Taha, M. H. Alham, and H. K. M. Youssef, "Multi-objective optimization for optimal allocation and coordination of wind and solar dgs, besss and capacitors in presence of demand response," *IEEE Access*, vol. 10, pp. 16 225–16 241, 2022. [Online]. Available: https://doi.org/10.1109/ACCESS.2022.3149135 ↑ 18

[40] L. H. Macedo, G. Muñoz-Delgado, J. Contreras, and R. Romero, "Optimal service restoration in active distribution networks considering microgrid formation and voltage control devices," *IEEE Trans. Ind. Appl.*, vol. 57, no. 6, pp. 5758–5771, 2021. [Online]. Available: https://doi.org/10.1109/TIA.2021.3116559 ↑ 18

Walter Gil-González

He received his BSc, MSc, and PhD degrees in Electrical Engineering from Universidad Tecnológica de Pereira (Colombia) in 2011, 2013, and 2019, respectively. He worked as an adjunct professor at Institución Universitaria Pascual Bravo. He is currently working as a professor in the Department of Electric Power Engineering, Universidad Tecnológica de Pereira. His research interests include power system control, stability, optimization, and operation.
Email: wjgil@utp.edu.co

Andrés Herrera-Orozco

He received BSc and MSc degrees in Electrical Engineering from Universidad Tecnológica de Pereira (Colombia) in 2010 and 2013, respectively, as well as a PhD from Universidade Federal do Rio Grande do Sul (Brazil) in 2017. He is currently a Professor at Department of Electrical Engineering School of Universidad Tecnológica de Pereira. He is a member of ICE3-UTP and CAFE-UTP research groups. His research interests include electrical smart grids, microgrid protection, power quality, fault analysis, and power systems analysis.
Email: arherrera@utp.edu.co

Alexander Molina-Cabrera

He received his BSc and MSc degrees in Electrical Engineering from Universidad Tecnológica de Pereira (Colombia) in 2004 and 2005. In 2018, he received a PhD from Universidad de los Andes (Colombia). He is currently the dean of the Engineering Faculty at Universidad Tecnológica de Pereira, where he also serves as an associate professor in the Department of Electric Power Engineering. His research focuses on nonlinear systems and power systems control and stability. Other areas of interest include artificial intelligence and electrical machines.
Email: almo@utp.edu.co